Journal of Solid State Chemistry **160,** 118–122 (2001)
doi:10.1006/jssc.2001.9202, available online at http://www.idealibrary.com on IDEAL®

The First Noncluster Vanadium(IV) Coordination Polymers: Solvothermal Syntheses, Crystal Structure, and Ion Exchange

Xian-Ming Zhang,* Ming-Liang Tong,* Hung Kay Lee,† and Xiao-Ming Chen*,[1]

* *School of Chemistry and Chemical Engineering, Zhongshan University, Guangzhou, 510275, People's Republic of China; and* † *Department of Chemistry, The Chinese University of Hong Kong, Shatin, New Territories, Hong Kong, People's Republic of China*
E-mail: cescxm@zsu.edu.cn

Received January 5, 2001; in revised form March 29, 2001; accepted April 9, 2001; published online July 3, 2001

Two isostructural vanadium(IV) coordination polymers $[VO(dod)_2]X_2$ [X = Cl, Br; dod = 1,4-diazoniabicyclo[2,2,2] octane-1,4-diacetate ($C_{10}H_{16}N_2O_4$)] have been synthesized solvothermally and determined by single-crystal X-ray analysis. Both of them crystallize in the tetragonal space group *P4/ncc* (no. 130), with cell parameters $a = 15.702(5)$, $c = 9.745(5)$ Å, $V = 2403(2)$ Å^3, $Z = 4$ for 1 and $a = 15.916(5)$, $c = 9.820(4)$ Å, $V = 2488(2)$ Å^3, $Z = 4$ for 2. In both complexes, each vanadium atom adopts a $V^{IV}O_5$ square-pyramidal environment, being coordinated by four oxygen atoms [V–O = 1.978(2) Å for 1 and 1.969(3) Å for 2] from four dod ligands and a terminal oxygen atom [V = O = 1.580(5) Å for 1 and 1.572(7) Å for 2]. The bis-monodentate dod ligands bridge vanadium atoms to furnish two-dimensional double wave-like layers of (4,4) topological type. Along the *c*-axis direction, there are square channels constructed from side-sharing saddle-shaped rings. The microporous material 1 shows chloride-to-sulfate exchange properties in aqueous media. © 2001 Academic Press

Key Words: **vanadium; coordination polymer; saddled-shape; ion exchange; solvothermal.**

INTRODUCTION

There has been extensive interest in organic–inorganic hybrid vanadium oxides, polyvanadate clusters, and vanadium complexes due to their structural aesthetics, catalysis, and magnetic properties as well as biological relevance (1–11). In contrast, the vanadium–organic coordination polymers via coordination of vanadium ions with bridging organic ligands remain rare. This may be attributed to vanadium at low-valence states having tendency to be oxidized and at high-valence states having tendency to form clusters. One may expect that microporous vanadium–organic coordination polymers with two- and three-dimensional frameworks will exhibit the potential applications, such as adsorption, ion exchange, and shape-selective catalysis, as documented for other metal–organic coordination polymers (12–19). Thus, the investigation to develop vanadium–organic coordination polymers is required for extension of the knowledge of the relevant structural types and for application as new materials. Surprisingly, only two structurally characterized vanadium–organic coordination polymers, namely, $[\{V(OH)(squarate)(H_2O)\}_2]$ and $[\{V(OH)(squarate)\}_2]\cdot 4H_2O$, have been reported to date, both of which are constructed from dimers of edging-sharing $V^{III}O_6$ octahedra (20). Neither vanadium(IV) nor vanadium(V) coordination polymers have been reported. It is believed that vanadium(IV) and vanadium(V) coordination polymers may be synthesized by judicious selection of ligands and reaction conditions. According to hard and soft acid and base theory, vanadium(IV) belongs to hard acid and has greater affinity to oxygen atoms than to nitrogen and sulfur atoms. Besides, it has also been known that the $[VO(H_2O)_4]^{2+}$ ions are major species of vanadium(IV) under acidic conditions, the four aqua ligands of which can be replaced by oxygen-donor ligands (21). Based on these considerations, we chose a bridging neutral zwitterionic ligand, 1,4-diazoniabicyclo[2,2,2]octane-1,4-diacetate (dod, a double betaine) (22), together with vanadium(V) oxide in aqueous ethanol to synthesize coordination polymers with the solvothermal method. Ethanol was chosen as solvent because it can reduce vanadium atoms from pentavalent to tetravalent at high temperature. We report herein two isostructural two-dimensional polymeric complexes $[VO(dod)_2]X_2$ (X = Cl, **1**, or Br, **2**), which represent the first noncluster vanadium(IV) coordination polymers.

EXPERIMENTAL

Syntheses

A mixture of V_2O_5 (0.09 g), dod·2HCl (0.10 g) or dod·2HBr (0.13 g), ethanol (2.80 g), and water (3.00 g) in the molar ratio 1:0.68:116:333 was stirred 30 min in air, then transferred, and sealed in a 23-cm^3 Teflon-lined stainless

[1] To whom correspondence should be addressed.

0022-4596/01 $35.00

container, which is heated to 180°C for 28 h and then cooled to room temperature at the rate of 5°C per hour. The products were filtered, washed with distilled water, and dried in air. Blue needle-like crystals **1** and **2** were recovered in approx. 35 and 40% yield based on dod, respectively.

Ion Exchange

A freshly prepared needle-like crystal of **1** (0.15 g) was immersed in the aqueous solution of Na_2SO_4 (0.5 M) for 5 h. The resulting product **3** (0.14 g) was filtered off, washed several times with distilled water, and dried in air. The transparency of the crystals was lost during immersion. Compound **3** was characterized by EA, IR spectra, and X-ray power diffraction (XRPD) patterns.

Physical Characterization

Elemental analyses were performed on a Perkin–Elmer 240 elemental analyzer and gave C = 40.58(40.42)%, H = 5.46(5.43)%, N = 9.38(9.43)% for **1**; C = 35.04(35.16)%, H = 4.67(4.72)%, N = 8.22(8.20)% for **2**; and C = 40.02(40.11)%, H = 5.48(5.39)%, N = 9.44(9.36)%, S = 1.06(0.96)% for **3**. The numbers in parentheses indicate the ideal calculated. The FT-IR spectra of **1**, **2**, and **3** were recorded from KBr pellets in the range 400–4000 cm^{-1} on a Nicolet 5DX spectrometer (Fig. 3). The recorded XRPD pattern of **3** was in agreement with the simulated one based on the single-crystal structure of **1** (Fig. 4). Thermal gravimetric analyses (TGA) were performed under static air atomosphere using a Perkin–Elmer 7 thermogravimetric analyzer with a heating rate of 10°C min^{-1}, which revealed that weight losses of approx. 78 and 83% for **1** and **2** occurred in the range 300–550°C. The EPR spectra of **1** were recorded with a Bruker spectrometer at 4 K, which showed a signal with anisotropic g factors, $g_x = 1.77$, $g_y = 1.99$, and $g_z = 2.23$.

Crystal Structure Determination

Data collection was performed at 293 K on a Siemens R3m diffractometer (Mo$K\alpha$, $\lambda = 0.71073$ Å). Lorentz-polarization and absorption corrections were applied. The structures were solved by direct methods (SHELXS-97) (23) and refined with full-matrix least-squares technique (SHELXL-97) (24). Analytical expressions of neutral-atom scattering factors were employed, and anomalous dispersion corrections were incorporated. In all cases, all nonhydrogen atoms were refined anisotropically and hydrogen atoms of organic ligands were geometrically placed. The crystallographic data for **1** and **2** are listed in Table 1. Atomic coordinates and equivalent isotropic displacement parameters and selected interatomic distances and angles for **1** and **2** are given in Tables 2 and 3.

TABLE 1
Crystal Data and Structure Refinement Parameters for 1 and 2

Empirical formula	$C_{20}H_{32}Cl_2N_4O_9V$	$C_{20}H_{32}Br_2N_4O_9V$
	1	**2**
Formula weight	594.34	683.26
Temperature (K)	293(2)	293(2)
Wavelength (Å)	0.71073	0.71073
Crystal system	Tetragonal	Tetragonal
Space group	*P4/ncc*	*P4/ncc*
a (Å)	15.702(5)	15.916(7)
b (Å)	15.702(5)	15.916(5)
c (Å)	9.745(5)	9.820(4)
V (Å^3)	2403(2)	2488(2)
Z	4	4
Density (calculated) (Mg/m^3)	1.643	1.824
Absorption coefficient (mm^{-1})	0.695	3.670
$F(000)$	1236	1380
Crystal size (mm)	$0.70 \times 0.42 \times 0.40$	$0.42 \times 0.15 \times 0.15$
θ range (°)	2.5–27.5	2.5–27.0
Reflections collected	2043	1584
Independent reflections	1387 ($R_{int} = 0.0623$)	1371 ($R_{int} = 0.0452$)
Absorption correction	Empirical	Empirical
Max. and min. transmission	0.768 and 0.713	0.720 and 0.628
Data/restrains/ parameters	1387/0/85	1371/0/85
Goodness-of-fit on F^2	1.036	1.027
Final R indices $[I > 2\sigma(I)]$	$R_1 = 0.0581$, w$R_2 = 0.1564$	$R_1 = 0.0510$, $wR_2 = 0.1049$
R indices (all data)	$R_1 = 0.0886$, w$R_2 = 0.1759$	$R_1 = 0.1075$, w$R_2 = 0.1246$

RESULTS AND DISCUSSION

Hydrothermal and solvothermal syntheses are relatively complex processes. Many factors can affect the reaction, such as initial reactants, concentration, pH, and crystallization temperature. In the syntheses of **1** and **2**, the choice of solvent and pH value of the reaction system were very important for the formation of the product. The ethanol molecule acts as not only a solvent but also as a reductive agent for vanadium from pentavalent to tetravalent. Attempts to prepare **1** and **2** in the absence of ethanol have proved to be unsuccessful. In addition, it has been found that an initial pH below 3 is also critical to the products.

X-ray structural analysis reveals that **1** and **2** are isostructural and consist of two-dimensional double wavelike layers of (4,4) topological type. Each vanadium atom in **1** and **2** adopts a $V^{IV}O_5$ square-pyramidal environment, being coordinated by four oxygen atoms [V–O = 1.978(2) Å for **1** and 1.969(3) Å for **2**] from four dod ligands and a terminal oxygen atom [V = O = 1.580(5) Å in **1** and 1.572(7) Å in **2**] (Fig. 1). It is known that the average V = O bond length of oxovanadium is approximately 1.6 Å, while the equatorial V–O bond length is in the range 1.8–2.1 Å. The average

TABLE 2
Atomic Coordinates ($\times 10^4$) and Isotropic Thermal Parameters ($\times 10^3$) for 1 and 2

Atom	x	y	z	U_{eq}
1 · Cl				
V(1)	7500	7500	504(1)	20(1)
O(1)	7500	7500	2125(5)	37(1)
O(2)	7438(2)	8697(2)	− 120(3)	31(1)
O(3)	8630(2)	9401(2)	448(2)	38(1)
C(1)	8048(2)	9218(2)	− 332(3)	27(1)
C(2)	7935(2)	9640(2)	− 1741(3)	30(1)
N(1)	8614(2)	10281(2)	− 2112(3)	23(1)
C(3)	8604(2)	11055(2)	− 1176(3)	25(1)
C(4)	8421(2)	10599(2)	− 3556(3)	26(1)
C(5)	9502(2)	9900(2)	− 2101(4)	26(1)
Cl(1)	6370(1)	11370(1)	− 2500	42(1)
2				
V(1)	7500	7500	434(2)	27(1)
Br(1)	6383(1)	11383(1)	− 2500	42(1)
O(1)	7500	7500	2034(8)	49(2)
O(2)	7465(2)	8674(2)	− 196(4)	39(1)
O(3)	8648(2)	9357(2)	395(4)	44(1)
C(1)	8076(3)	9189(3)	− 393(6)	34(1)
C(2)	7994(3)	9607(3)	− 1778(5)	36(1)
N(1)	8655(2)	10248(2)	− 2130(4)	25(1)
C(3)	8630(3)	11004(3)	− 1200(5)	32(1)
C(4)	8479(3)	10573(3)	− 3566(5)	29(1)
C(5)	9531(3)	9877(3)	− 2127(5)	31(1)

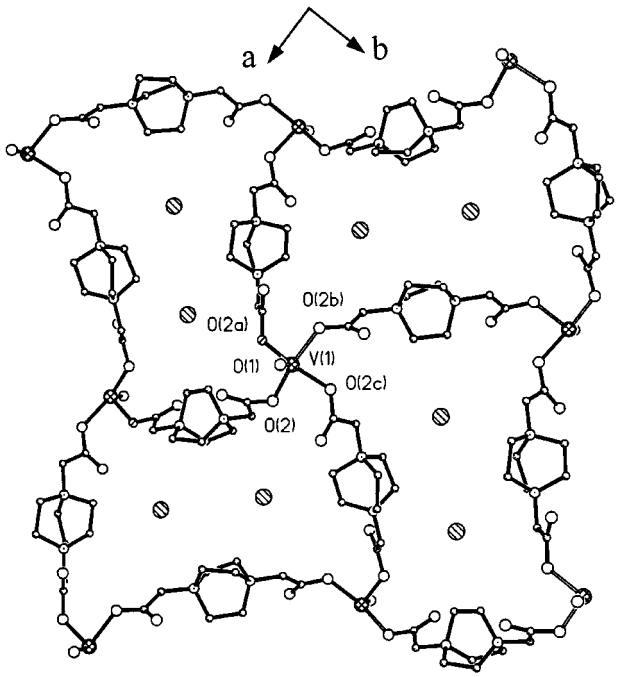

FIG. 1. Perspective plot of the two-dimensional structure of **1** viewed along the c axis.

lengths of 1.576 Å for V = O and 1.974 Å for V–O bonds in **1** and **2** indicate the vanadium atoms have a typical square-pyramidal arrangement. It should be particularly noted that the coordination mode of dod in **1** and **2** differs from both chelating and bridging coordination modes of squarate that are supposed to be the reason of stabilization of $[\{V(OH)(squarate)(H_2O)\}_2]$ and $[\{V(OH)(squarate)\}_2]\cdot 4H_2O$ (20). Each dod ligand covalently coordinates in a bis-monodentate μ_2-mode to two vanadium atoms and the propagation of the array results in wave-like chains along the [110] direction. Similar to this, wave-like chains running along the [1$\bar{1}$0] direction are produced by interconnection of vanadium atoms and dod ligands. The intercrossings at vanadium sites of chains along the [110] and [1$\bar{1}$0] directions give rise to a double wave-like two-dimensional layer. The basic motif of a two-dimensional layer is saddle-shaped rings of size approx. 12.0×6.2 Å that are enclosed by 44 atoms, including four vanadium atoms. The guest Cl^- or Br^- ions reside on the saddle-shaped rings to maintain the charged neutrality. Alternately, the double wave-like two-dimensional layer may be viewed as an array constructed from side-sharing saddle-shaped rings, where the terminal oxygen atoms alternately are oriented up and down. Recently one similar polymeric structural motif was documented in $[Cu_5(bpp)_8(SO_4)_4(EtOH)(H_2O)_5](SO_4)\cdot EtOH\cdot 25{\cdot}5\,H_2O$ (25). However, the three-dimensional stacking arrays of **1** and **2** are quite different from the copper(II) complex. As shown in Fig. 2, the layers of **1** and **2** stack in a staggered fashion with interlayer V ⋯ V separations of 4.87 Å for **1** and 4.91 Å for **2**, which repeat with an $\cdots ABABAB \cdots$ sequence. In the copper(II) complex the layered motifs are entangled with the other type of polymeric motifs (ribbons) into a three-dimensional array. In addition, it is noteworthy that there is weak interaction between interlayer V(1) and O(1) atoms with a V ⋯ O distance of 3.29 Å, which may play an important role in stabilization of **1** and **2**, as shown by the dashed

TABLE 3
Selected Bond Length (Å) and Bond Angles (°) for 1 and 2

	1	**2**
V(1)–O(1)	1.580(5)	1.572(7)
V(1)–O(2)	1.978(2)	1.969(3)
O(2)–C(1)	1.276(4)	1.287(6)
O(3)–C(1)	1.223(4)	1.224(6)
O(1)–V(1)–O(2a)	107.9(1)	108.3(1)
O(2a)–V(1)–O(2b)	84.58(5)	84.35(7)
O(2a)–V(1)–O(2c)	144.2(2)	143.4(2)
C(1)–O(2)–V(1)	128.4(2)	129.1(4)
O(3)–C(1)–O(2)	127.7(3)	127.3(5)

Note. Symmetry codes: (a) y, 1.5 − x, z; (b) 1.5 − x, 1.5 − y, z; (c) 1.5 − y, x, z.

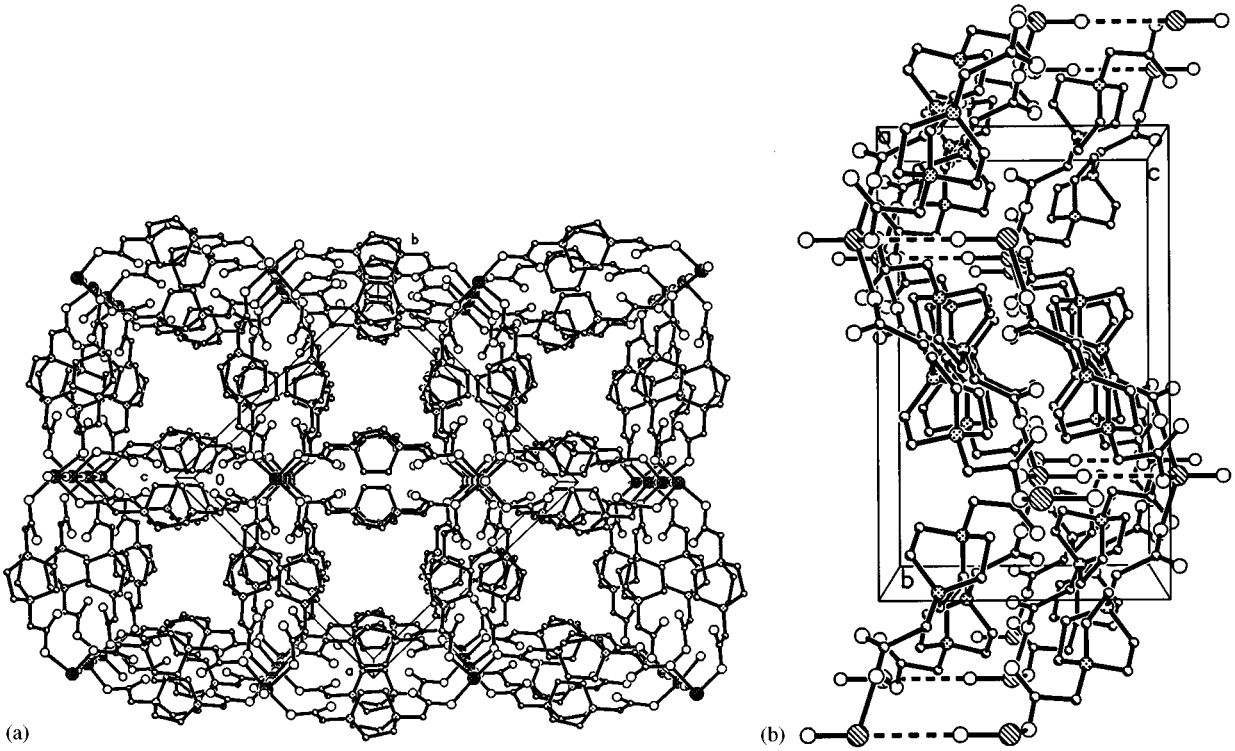

FIG. 2. The three-dimensional stacking array of **1** viewed along (a) the *c* axis and (b) the a axis. For clarity, the chloride ions are omitted.

lines in Fig. 2b. Fortunately, the staggered stacking does not cover all voids but leaves square channels running along the *c*-axis direction (approx. 6.2×6.2 Å^2), which provide the path for guest ions entering into or coming out the lattice.

Compounds **1** and **2** exhibit virtually identical IR spectra, as shown in Fig. 3a. The strong band at 1666 cm^{-1} is consistent with the stretching vibration of carboxylate and the peak at 986 cm^{-1} is characteristic of the V = O stretching vibration. The powdered EPR spectra show a signal with anisotropic g factors ($g_x = 1.77$, $g_y = 1.99$, and

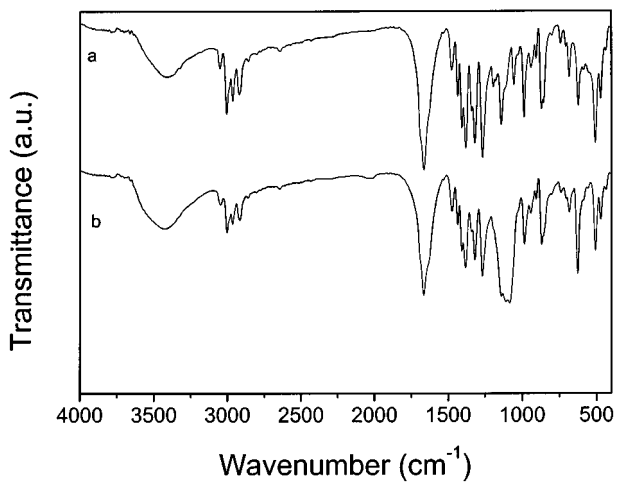

FIG. 3. IR spectra of (a) **1** and (b) its exchanged product **3**.

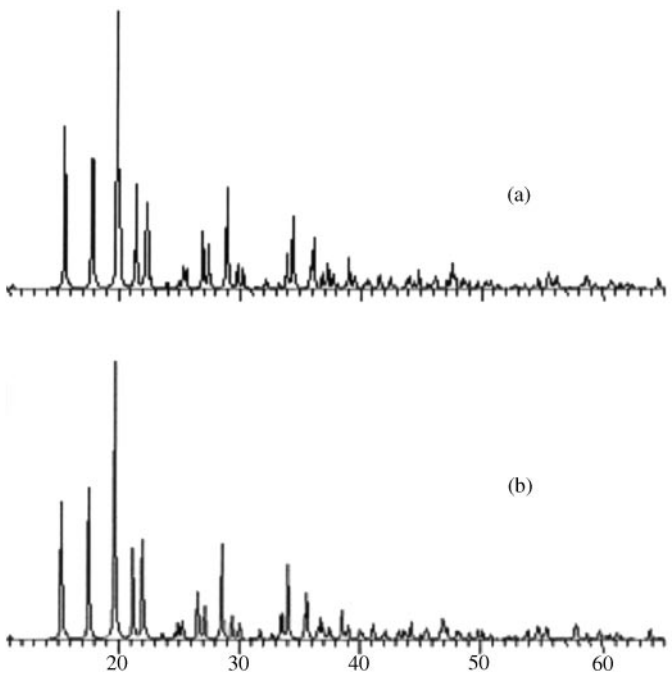

FIG. 4. (a) Simulated XRPD pattern of **1** and (b) measured XRPD pattern of **3**.

$g_z = 2.23$), confirming that the oxidation state of vanadium atoms are tetravalent (26).

An ion exchange test of **1** was carried out and the exchanged product **3** was identified by IR spectroscopy, elemental analysis, and XRPD. The IR spectrum of **3** (Fig. 3b) shows a strong band at 1107 cm^{-1}, corresponding to free SO_4^{2-}, compared with that of **1**. The XRPD pattern of **3** (Fig. 4) is very similar to the simulated one based on the single-crystal structure of **1**, which indicates no skeleton collapse during the ion-exchange course. Elemental analysis shows that ion exchange yield is approx. 18% and extension of exchange time from 5 to 9 h does not apparently improve the exchange yield. The lower exchange yield may be attributed to the fact that there are only one-directional channels in **1** running along the *c*-axis direction, and SO_4^{2-} and Cl^- ions are hard to pass through the channels because of the medium pore size and mutual collision of the two kinds of ions.

ACKNOWLEDGMENTS

This work was supported by the National Natural Science Foundation of China (No. 29971033) and the Ministry of Education of China.

REFERENCES

1. T. Chirayil, P. Y. Zavalij, and M. S. Whittingham, *Chem. Mater.* **10,** 2629 (1998).
2. P. J. Hagrman, D. Hagrman, and J. Zubieta, *Angew. Chem. Int. Ed.* **38,** 2638 (1999).
3. B. E. Koene, N. J. Taylor, and L. F. Nazar, *Angew. Chem. Int. Ed.* **38,** 2888 (1999).
4. Z. Shi, S.-H. Feng, S. Gao, L.-R. Zhang, G.-Y. Yang, and J. Hua, *Angew. Chem. Int. Ed.* **39,** 2325 (2000).
5. L. C. W. Baker and D. C. Glick, *Chem. Rev.* **98,** 3 (1998).
6. P. Gouzerh and A. Proust, *Chem. Rev.* **98,** 77 (1998).
7. D. Rehder, *Angew. Chem. Int. Ed. Engl.* **30,** 148 (1991).
8. M. A. Pepera, J. L. Callahan, M. J. Desmond, E. C. Milberger, P. R. Blum, and N. J. Bremer, *J. Am. Chem. Soc.* **107,** 4883 (1985).
9. G. Centi, F. Trifiro, J. R. Ebner, and V. M. Franchetti, *Chem. Rev.* **88,** 55 (1988).
10. M. T. Pope and A. Müller, *Angew. Chem. Int. Ed. Engl.* **30,** 34 (1991).
11. S. L. Castro, Z.-M. Sun, C. M. Grant, J. C. Bollinger, D. N. Hendrickson, and G. Christou, *J. Am. Chem. Soc.* **120,** 2365 (1998).
12. A. K. Cheetham, G. Ferey, and T. Loiseau, *Angew. Chem. Int. Ed.* **38,** 3268 (1999).
13. O. M. Yaghi, H. Li, C. Davis, D. Richarson, and T. L. Groy, *Acc. Chem. Res.* **31,** 474 (1998).
14. C. Janiak, *Angew. Chem. Int. Ed. Engl.* **36,** 1431 (1997).
15. M. J. Zaworotko, *Chem. Soc. Rev.* **23,** 283 (1994).
16. K. S. Min and M. P. Suh, *J. Am. Chem. Soc.* **122,** 6834 (2000).
17. H. Li, M. Eddaoudi, M. O'Keeffe, and O. M. Yaghi, *Nature* **402,** 276 (1999).
18. M. Fujita, M. Aoyagi, F. Ibukuro, K. Ogura, and K. Yamaguchi, *J. Am. Chem. Soc.* **120,** 611 (1998).
19. B. F. Abrahams, B. F. Hoskins, D. M. Michail, and R. Robson, *Nature* **369,** 727 (1994).
20. K.-J. Lin and K.-H. Lii, *Angew. Chem. Int. Ed. Engl.* **36,** 2076 (1997).
21. F. A. Cotton, "Advanced Inorganic Chemistry," p. 671. Wiley, New York, 1988.
22. P.-R. Wei, D.-D. Wu, B.-M. Wu, and T. C. W. Mak, *Aust. J. Chem.* **50,** 85 (1997).
23. G. M. Sheldrick, "SHELXS-97, Program for X-Ray Crystal Structure Solution." University of Göttingen: Göttingen, Germany, 1997.
24. G. M. Sheldrick, "SHELXS-97, Program of X-Ray Crystal Structure Refinement." University of Göttingen: Göttingen, Germany, 1997.
25. L. Carlucci, G. Ciani, M. Moret, D. M. Proserpio, and S. Rizzato, *Angew. Chem. Int. Ed.* **39,** 1506 (2000).
26. G. R. Hanson, Y. Sun, and C. Orvig, *Inorg. Chem.* **35,** 6507 (1996).